DOI: 10.38061/idunas.1363477

IDUNAS	NATURAL & APPLIED SCIENCES JOURNAL	2023 Vol. 6 No. 2 (49-60)

Determination of the CO_2 Laser Parameters on Dimple Geometry on Al_2O_3 Ceramic Surface

Research Article

Çağla Pilavcı[1,4*], Satılmış Ürgün[3*], Yasemin Tabak[2*], Timur Canel[4*]

[1]TUBITAK Marmara Research Center Life Sciences, Kocaeli, Türkiye

[2]TUBITAK Marmara Research Center Material Technologies, Kocaeli, Türkiye

[3] Faculty of Aeronautics and Astronautics, Department of Aviation Electrics and Electronics, Kocaeli University, Kocaeli, Türkiye.

[4] Department of Physics, Faculty of Arts and Science, Kocaeli University, 41380, Kocaeli, Türkiye

Author E-mails:
cagla.pilavci@gmail.com
urgun@kocaeli.edu.tr
yasemin.tabak@tubitak.gov.tr
tcanel@kocaeli.edu.tr
Ç. Pilavcı ORCID ID: 0009-0005-5237-9598
S. Ürgün ORCID ID: 0000-0003-3889-6909
Y. Tabak ORCID ID: 0000-0002-4912-8828
T. Canel ORCID ID: 0000-0002-4282-1806

*Correspondence to: Çağla Pilavcı, TUBITAK Marmara Research Center Life Sciences, Kocaeli, Türkiye
DOI: 10.38061/idunas.1363477

Received: 20.09.2023; Accepted: 06.12.2023

Abstract

Dimples on Al_2O_3 ceramic plates were created with a CO_2 laser using different laser parameters. The effects of the laser parameters used on the dimple geometry were investigated and the necessary laser parameters were optimized to obtain the desired dimple geometry. Taguchi method was used in the optimization process. The effects of laser power, scan speed and laser frequency from laser parameters were investigated. Optimum laser parameters were determined as a result of the Taguchi Optimization method. In addition, the laser parameter with the highest effect on the result was determined. Optimum laser parameters were obtained as 60 W for laser power, 35 s for laser exposure duration and 50 kHz for laser frequency.
Keywords: Al2O3, Ceramics, Optimization, Laser texturing, Laser parameters.

1. INTRODUCTION

Aluminum oxide, commonly known as Al_2O_3, is a versatile ceramic material with a wide range of applications in various industries (Sarkar et al., 2004). Its unique combination of exceptional mechanical, thermal, and electrical properties make it an ideal choice for numerous high-performance applications. Al_2O_3 ceramics are characterized by their high hardness, excellent wear resistance, and outstanding

corrosion resistance, making them suitable for use in harsh environments where other materials might fail. These ceramics are composed of a stable crystal structure, primarily consisting of corundum, which contributes to their remarkable stability and robustness.

One of the most notable properties of Al_2O_3 ceramics is their exceptional thermal resistance. With a melting point of approximately 2050°C, Al_2O_3 exhibits remarkable thermal stability, making it an ideal material for high-temperature applications. Additionally, its low thermal expansion coefficient ensures minimal dimensional changes under varying temperatures, reducing the risk of thermal stress-induced failures. As a result, Al_2O_3 ceramics find extensive use in industries, such as aerospace, metallurgy, and manufacturing, where high-temperature processes and demanding thermal conditions are prevalent [37].

Apart from its exceptional mechanical and thermal properties, Al_2O_3 ceramics possess excellent dielectric and insulating characteristics [48]. This makes them highly desirable for electronic and electrical applications, including semiconductor packaging, high-power electrical insulators, and substrates for microelectronics. Their ability to withstand high voltages and resist electrical breakdown allows for efficient and reliable operation in demanding electrical environments. Moreover, Al_2O_3 ceramics can be tailored for specific electrical properties through dopants, offering engineers and researchers a degree of flexibility in designing electronic components.

In the biomedical field, Al_2O_3 ceramics have garnered considerable attention for their biocompatibility and bio-inertness. When used as medical implants or prosthetics, Al_2O_3 ceramics exhibit excellent resistance to chemical reactions with body fluids and tissues, ensuring minimal adverse reactions. Furthermore, their high strength and wear resistance make them suitable for load-bearing applications in orthopedics and dentistry [34]. The biocompatibility, combined with the material's inert nature, contributes to its widespread use in hip joint replacements, dental implants, and other medical devices.

Despite the numerous advantages, Al_2O_3 ceramics do present some challenges in their fabrication and processing. The material's high hardness can make shaping and machining difficult, requiring specialized manufacturing techniques, such as diamond grinding or laser cutting. Additionally, the inherent brittleness of ceramics poses concerns for their fracture toughness, which must be carefully considered in structural applications subjected to impact or dynamic loading [5]. Researchers continue to explore various techniques, including sintering additives and advanced processing methods, to enhance the fracture toughness and overall mechanical performance of Al_2O_3 ceramics.

In conclusion, Al_2O_3 ceramics stand as a remarkable class of materials with diverse applications across numerous industries. Their exceptional properties, including high hardness, thermal stability, electrical insulation, and biocompatibility, make them indispensable in a wide range of critical applications. As researchers and engineers push the boundaries of material science, continued advancements in processing techniques and material design hold the promise of unlocking even more potential for Al_2O_3 ceramics in the future.

Laser surface texturing is a cutting-edge technique used to modify the surface topography of materials through controlled laser ablation [24]. This involves the precise application of laser energy to create micro or nano-scale patterns, roughness, or features on the surface. The fundamental principle behind laser surface texturing lies in the interaction of the laser beam with the material, which leads to localized melting, vaporization, or solid-state phase changes. The resulting surface textures offer a myriad of advantages, including improved tribological properties, enhanced wettability, reduced friction, and tailored optical characteristics. As a versatile and non-contact method, laser surface texturing has gained widespread attention in various industries, from automotive and aerospace to biomedical and energy sectors.

One of the key benefits of laser surface texturing is its ability to tailor surface properties based on specific requirements. By adjusting laser parameters, such as pulse duration, energy density, and spot size, engineers can precisely control the depth, shape, and spatial distribution of the textured features. For instance, in the automotive industry, laser texturing has been applied to engine cylinder walls to create specific patterns that improve oil retention and reduce friction, leading to enhanced fuel efficiency and

reduced emissions [9, 40]. In the field of microfluidics, laser-textured channels have been utilized to control fluid flow and optimize mixing, offering novel solutions for lab-on-a-chip devices and microreactors.

The influence of laser wavelength and material characteristics on the surface texturing process cannot be overlooked. Different materials exhibit varying responses to laser energy, affecting the ablation mechanism and resulting surface features. Metals, ceramics, polymers, and even transparent materials can be textured using lasers with appropriate wavelengths and pulse characteristics[30]. Moreover, advances in ultrafast laser technology have enabled the creation of sub-wavelength surface structures, leading to unique optical properties, such as antireflection and light-trapping effects. These developments have opened up exciting possibilities for photovoltaic applications and laser-induced periodic surface structures (LIPSS) in photonics.

However, challenges remain in the widespread adoption of laser surface texturing. The process demands precise control and stability of laser parameters to achieve consistent and repeatable results. Additionally, the high-power laser systems required for certain applications can be costly, limiting accessibility for some industries. Furthermore, the impact of laser-induced heat on the material's mechanical properties and potential surface damage necessitates a comprehensive understanding of the material's response to laser energy. To address these concerns, ongoing research efforts are focused on optimizing laser texturing techniques, developing cost-effective systems, and investigating new materials suitable for laser texturing.

In conclusion, laser surface texturing has emerged as a powerful tool for surface modification, offering a wide range of possibilities for improving material performance and tailoring surface characteristics to meet specific application requirements. From enhancing the efficiency of mechanical systems to revolutionizing optical devices and microfluidics, the versatility of laser surface texturing holds significant promise for various industrial sectors. As research continues to advance, and technology becomes more accessible, the field of laser surface texturing is likely to witness even greater innovation and integration into diverse fields of science and engineering.

Surface patterns play a crucial role in determining the mechanical and tribological properties of materials [43]. By altering the topographical features at the micro and nano scales, surface patterns can significantly affect the friction, wear resistance, and mechanical behavior of materials. The interaction between contacting surfaces is governed by these surface patterns, and their influence is of particular importance in engineering applications where reducing friction and wear is essential for improving the overall performance and lifespan of components. Understanding the relationship between surface patterns and mechanical/tribological properties is pivotal for tailoring materials to meet specific functional requirements across various industries.

The topographical characteristics of a surface pattern directly influence its mechanical properties. The presence of micro-scale asperities, such as surface roughness, can enhance the interlocking between contacting surfaces, increasing the load-bearing capacity and overall strength of the material. In contrast, nano-scale surface patterns, nanoindentations, or nanocavities, can introduce stress concentration sites, affecting the material's fracture toughness and fatigue resistance. Additionally, the distribution and arrangement of surface patterns significantly impact the contact area and stress distribution during loading, which in turn affects the material's deformation behavior, hardness, and elastic modulus.

Surface patterns also exert a profound influence on the tribological properties of materials, especially in sliding and rolling contact scenarios. The creation of specific surface textures can reduce friction and wear rates by promoting the formation of a lubricating film, trapping wear debris, or facilitating hydrodynamic lubrication [13]. In some cases, laser-textured surfaces with controlled roughness have shown improved boundary lubrication properties, leading to reduced friction and enhanced wear resistance. Moreover, the presence of well-defined surface patterns can alter the coefficient of friction and wear mechanisms, allowing for tailored solutions based on specific application requirements.

The effect of surface patterns on mechanical and tribological properties is highly dependent on the material's composition and the nature of the applied loads. For example, in metal alloys, surface patterns

can lead to strain-hardening effects, where localized plastic deformation strengthens the material near the surface. However, in brittle materials like ceramics, surface patterns can exacerbate crack initiation and propagation, leading to reduced wear resistance. Understanding the trade-offs and limitations associated with different surface patterns is crucial for selecting the most appropriate texture for a given application.

In conclusion, surface patterns play a vital role in determining materials' mechanical and tribological properties. Their influence extends to various aspects, such as load-bearing capacity, friction, wear resistance, and deformation behavior. By carefully designing and controlling surface patterns, engineers can tailor the properties of materials to achieve desired outcomes in specific applications. The optimization of surface patterns holds significant potential for improving the efficiency and reliability of engineering systems, making it a topic of ongoing research and exploration in the fields of material science and surface engineering.

In this study, laser beams with different laser power and different exposure time were sent on the Al_2O_3 ceramic surface. Images of the cavities were taken with a high-resolution microscope to examine the effect of laser power and the effect of laser exposure time on the cavity sizes. Cavity sizes were measured using the images obtained.

Optimization methods are mathematical and computational methods that aim to find the best or non-worst values of an objective function under certain constraints. In general, optimization methods attempt to optimize an objective function (usually a maximum or minimum) by adjusting the values of variables in a given problem. Such methods are used in many different fields and disciplines, such as Engineering, Economics, Data Mining and Machine Learning, Transport and Logistics, Energy Management, and Healthcare, in addition to scientific research. Optimization methods may include different types of techniques, usually mathematical algorithms, heuristics, or meta-heuristics. These methods may require different approaches depending on the nature, size, and complexity of the problem. The most widely used optimization algorithms include gradient-based methods, genetic algorithms, simulation-based optimization, surface response methodology, etc.

The Taguchi Method, developed by Dr. Genichi Taguchi, is a reliable method for designing experiments and optimizing parameters, which is widely used in engineering and scientific studies. This method, which is a product of statistical science, provides a systematic approach to optimize multi-parameter systems. The main objective of the Taguchi Method is to optimize a smaller number of parameters.

In the Taguchi Method, one of the three basic elements is the controllable factors called "signal", i.e. parameters. The second is the so-called "noise", which is uncontrollable, i.e. undesirable. The third element is what is aimed as a result of the experiments. Although the objective is usually a numerical value, in some cases it may be a non-numerical parameter. In the Taguchi method, the parameter is numerical and orthogonal arrays are designed according to the number of levels of each parameter. According to these orthogonal arrays, experimental sets and the number of experiments are determined. The Taguchi method not only minimizes the time and resources required for the experiment but also ensures the robustness and reliability of the results obtained. The optimization process involves maximizing the S/N ratio to improve the desired characteristics of the system while minimizing sensitivity to noise factors.

2. MATERIALS & METHODS

In this study, dimples were formed using a CO_2 laser on 10 mm thick Al_2O_3 ceramic plates prepared at TUBITAK Marmara Research Center. The wavelength of the CO_2 laser used is 10600 μ and the maximum power is 130 watts. The effects of laser power and laser exposure time on the dimple geometry were investigated. Laser beams with different laser power and different frequency were sent at different times on Al_2O_3 ceramic plates. The levels of the analyzed parameters are given in Table 1.

Table 1. Parameters and Levels.

	1st level	2nd level	3th level
Power (W)	40	80	120
Exposure Time (s)	5	20	35
Frequency (kHz)	5	25	50

In experiments with classical experimental designs, 3^3=27 experiments are required to examine the effect of each parameter on the result. Taguchi method offers different solutions, such as the relationship between parameters or which parameter is more effective, as well as obtaining the same result with fewer experiments. By performing fewer experiments, both the material used, and time are saved.

According to Taguchi, experimental design, the optimum parameter levels can be determined by using the L_9 orthogonal index. Experimental sets designed according to the L_9 orthogonal index are given in Table 2.

Table 2. Parameter and Levels.

Parameters → / Exp. Sets ↓	Power (W)	Time (s)	Frequency (kHz)
1	30	5	5
2	30	20	25
3	30	35	50
4	60	5	25
5	60	20	50
6	60	35	5
7	90	5	50
8	90	20	5
9	90	35	25

When the laser power was less than 30 W, no cavity formation was observed on the ceramic material. When the laser power was greater than 90 W, uncontrollable deformation occurred due to overheating. Similarly, cavity formation was not observed at low power values when the laser exposure time was less than 5 seconds. When the laser exposure time was 35 seconds, excessive thermal deformation occurred due to the excessive amount of energy transferred to the material. When the frequency was more than 50 kHz, the frequency was limited to 50 kHz since no visible difference could be obtained.

With the 3 parameters used and 3 levels of each of these parameters, 27 experiments should be done with classical test methods. However, with the Taguchi optimization method, the same result can be obtained with 9 experiments and 1 confirmation experiment with a total of 9 experiments.
According to the Taguchi method, the target must be defined first. There can be three different targets. There is a separate calculation method for each target. These; quality in Taguchi Design of Experiment method the criterion used in measuring and evaluating the characteristics is the ratio of signal (S) to noise factor (N). The signal value is the value given by the system and desired to be measured. The real value and the noise factor are the measured values. Represents the share of undesirable factors in it does. Experiments in calculating the signal/noise ratio and the quality value targeted to be achieved as a result feature is also important. There are three important categories;

1) Larger the Better

$$S/_{N_i} = -10log_{10}\left[\frac{1}{n}\sum_{i=1}^{n}\frac{1}{y_i^2}\right] \quad (1)$$

2) Smaller the Better

$$S/_{N_i} = -10log_{10}\left[\frac{1}{n}\sum_{i=1}^{n}y_i^2\right] \quad (2)$$

3) Nominal the Best

$$S/_{N_i} = -10log_{10}\left[\frac{1}{n}\sum_{i=1}^{n}(y_i - m)^2\right] \quad (3)$$

In these equations, n is the number of trials, y_i is the measurement result, and m is the target value. The Taguchi method suggests an L_9 orthogonal array for 3 parameters and 3 levels. Experimental sets according to the L_9 orthogonal index are given in Table 2.

3. RESULTS & DISCUSSION

Figure 1 shows the micro-sized dimples obtained with each set of experiments. The cavity diameters and Heat Affected Zone diameters of the dimples were measured using the images obtained. The ratio of the diameters of the dimples to the HAZ diameters was considered to be the best. In other words, the aim of this experiment is to have the highest ratio of the cavity size to the HAZ size when the Heat Affected Zone size is compared with the cavity size. Accordingly, "Larger the better" characteristic was used when calculating the S/N ratio. In order to minimize the error rate in the experiments, 3 repetitions of each set of experiments were performed. The measurement results, calculated ratios, and S/N ratios obtained using these ratios are given in Table 3.

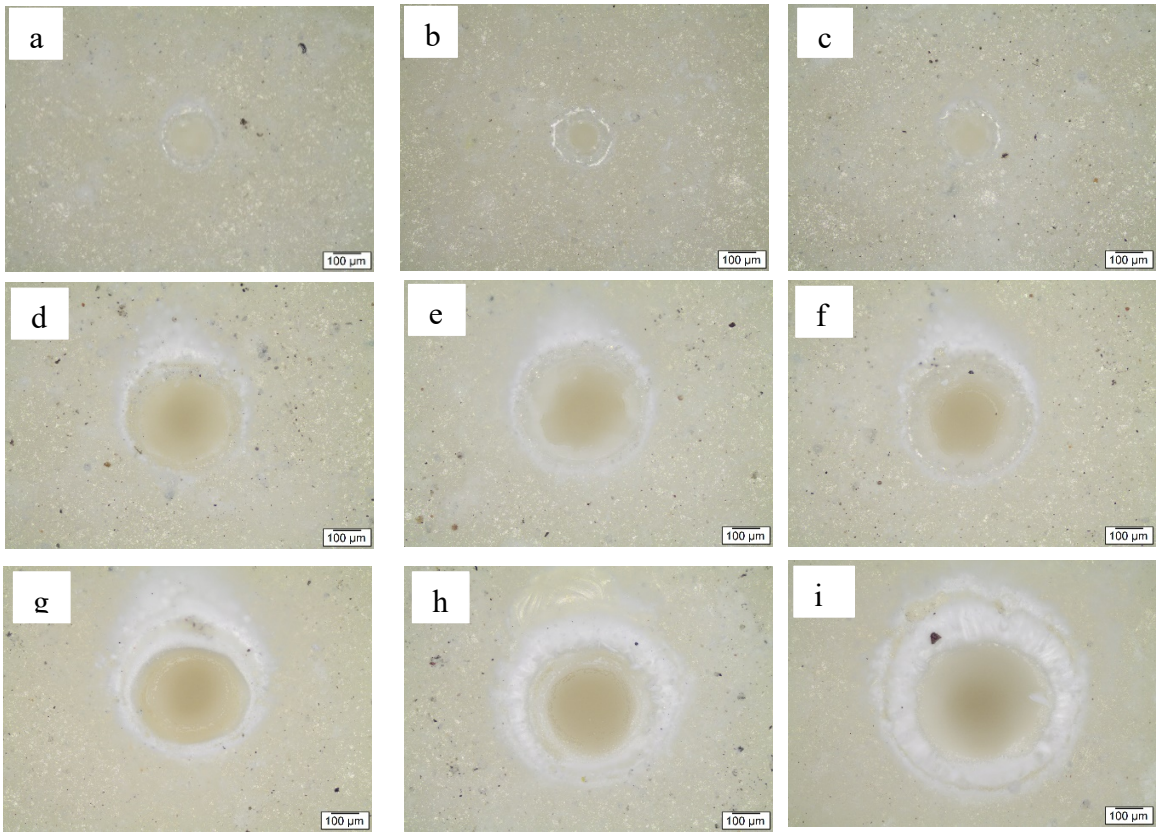

Figure 1. Optical microscope images of dimples obtained with the experimental sets in Table 2. (a) Experimental set number 1, (b) Experimental set number 2, (c) Experimental set number 3, (d) Experimental set number 4, (e) Experimental set number 5, (f) Experimental set number 6, (g) Experimental set number 7, (h) Experimental set number 8, (i) Experimental set number 9.

Table 3. Size ratios of three measurements with calculated S/N ratios. Cavity diameter to HAZ diameter Ratio of Dimple.

	1st	2nd	3rd	S/N
1	0,54	0,70	0,74	-3,86
2	0,57	0,50	0,68	-4,87
3	0,68	0,68	0,57	-3,87
4	0,74	0,71	0,67	-3,06
5	0,70	0,74	0,75	-2,70
6	0,66	0,73	0,67	-3,29
7	0,65	0,65	0,68	-3,58
8	0,90	0,59	0,72	-3,03
9	0,68	0,70	0,82	-2,79

In addition to finding the optimum parameters, the Taguchi method can also calculate how much the parameters used affect the result. The sum of squares (SST) indicates the variance of S/N [3].

$$SS_T = \sum_{i=1}^{n} (\eta_i - \eta_m)^2. \quad (4)$$

The SST value is actually the sum of the squares of each factor ($SS_T=SS_A+SS_B+SS_C$), and it can also be obtained by equation (4) as

$$SS_A = \sum_{i=1}^{k_A} n_{Ai}(\eta_{Ai} - \eta_m)^2. \quad (5)$$

Table 4 was obtained by using the data in Table 3, equation (4) and equation (5).

Table 4. ANOVA table for Optimum Ratio of Dimple diameter to HAZ diameter.

	Average S/N					
	1st level	2nd level	3rd level	Degree of Freedom	Effect Rate	Optimum Parameters
Power (W)	-4,20	-3,02	-3,13	2	94,44	60 W
Exposure Time (s)	-3,50	-3,53	-3,32	2	2,93	35 s
Frequency (kHz)	-3,39	-3,58	-3,38	2	2,63	50 kHz
Total		-3,45			100	
Optimum S/N						-2,82
Optimum Ratio of Dimple diameter to HAZ diameter						0,72

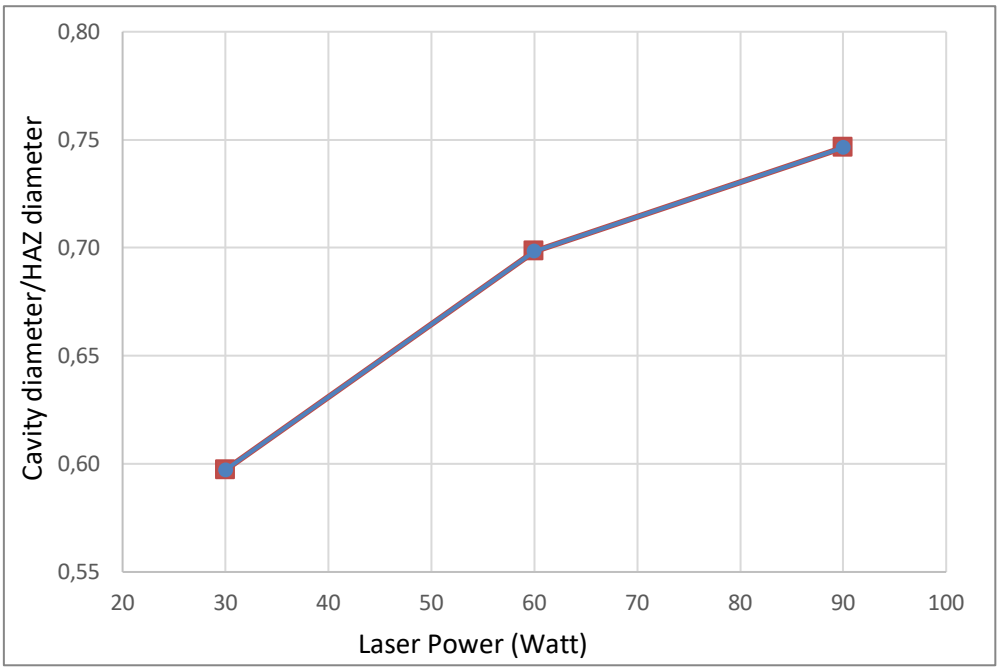

Figure 2. Main effect plot for laser power on the ratio of cavity diameter to HAZ diameter.

As can be seen in the Main effect plot for laser power, when the laser power is increased from 30 W to 60 W, the ratio of widths increases. However, when the speed was increased from 60 W to 90 W, the width ratio also increased but slower than the previous stage. The highest ratio was observed when the laser power was 90 W.

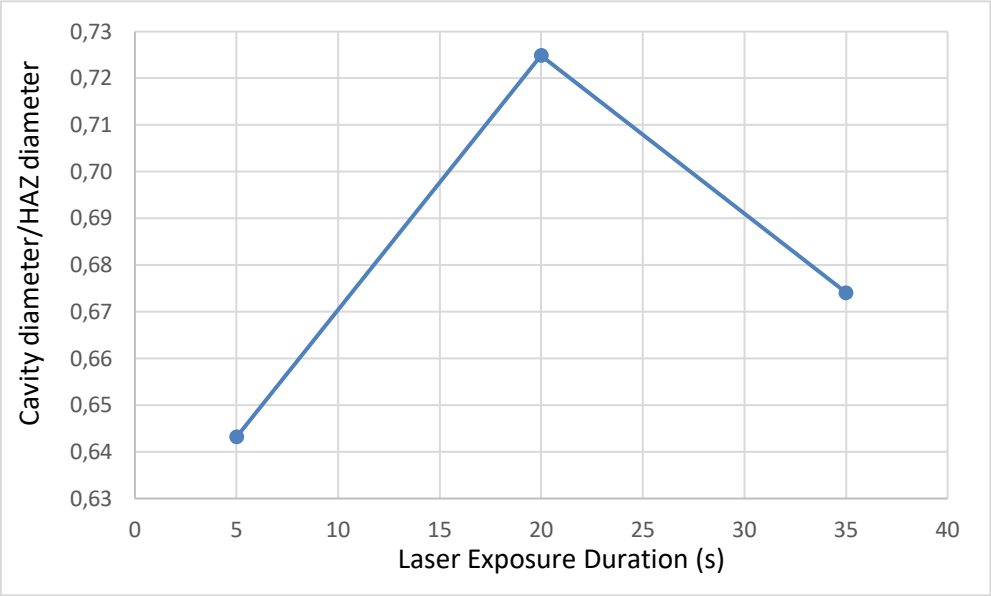

Figure 3. Main effect plot for laser exposure duration on the ratio of cavity diameter to HAZ diameter.

As seen in the Main effect plot for Laser exposure duration, when the Laser exposure duration is increased from 5 s to 20 s, the ratio of widths increases. However, when the Laser exposure duration is increased from 20 s to 35 s, the ratio of widths decreases. The highest ratio was observed when the Laser exposure duration was 20 s.

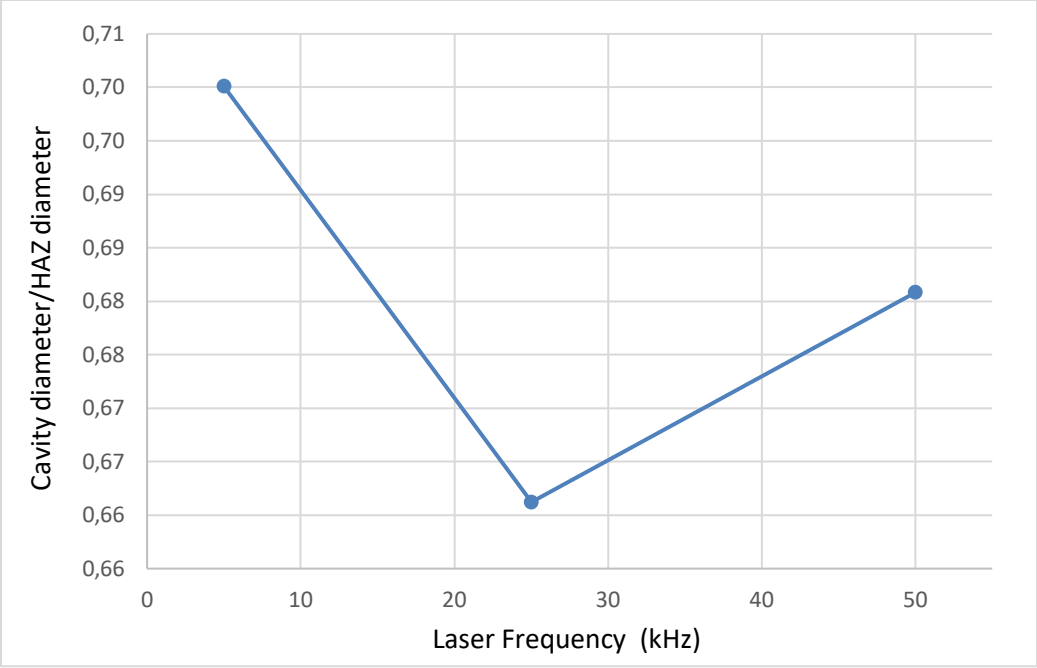

Figure 4. Main effect plot for laser frequency on the ratio of cavity diameter to HAZ diameter.
As seen in the Main effect plot for laser frequency, when the laser frequency is increased from 5 kHz to 25 kHz, the ratio of the widths decreases. However, when the frequency is increased from 25 kHz to 50 kHz, the width ratio increases. The highest ratio was observed when the frequency was 5 kHz.

4. CONCLUSION

The Taguchi method was applied to achieve two objectives: optimizing the size of the largest possible cavity and minimizing the width of the heat-affected zone adjacent to this cavity. Optimum laser parameters were obtained as 60 W for laser power, 35 s for laser exposure duration, and 50 kHz for laser frequency. In addition, among the parameters analyzed in order to reach the desired result, the parameter that affected the result the most was calculated as laser power with a rate of 94.44%. The rate of laser exposure duration and laser frequency affecting the result is quite low. Laser exposure duration and laser frequency affected the result by 2.93% and 2.63% respectively.

REFERENCES

1. Alhassan, I., Gashua, A. G., Sunday, D. O. G. O., & Mahmud, S. A. N. İ. (2018). Physical properties and organic matter content of the soils of Bade in Yobe State, Nigeria. International Journal of Agriculture Environment and Food Sciences, 2(4), 160-163.

2. Arshad, M. A., Lowery, B., & Grossman, B. (1997). Physical tests for monitoring soil quality. Methods for assessing soil quality, 49, 123-141.5. Bhatt, R. (2019). Importance of Soil Texture. (retrieved from https://www.scribd.com on 30 December 2019)

3. Canel, T., Kaya, A. U., & Celik, B. (2012). Parameter optimization of nanosecond laser for microdrilling on PVC by Taguchi method. Optics & Laser Technology, 44(8), 2347-2353.

4. Chaudhari, P. R., Ahire, D. V., Ahire, V. D., Chkravarty, M., & Maity, S. (2013). Soil bulk density as related to soil texture, organic matter content and available total nutrients of Coimbatore soil. International Journal of Scientific and Research Publications, 3(2), 1-8.

5. Chu, B., Liu, Q., Liu, L., Lai, X., & Mei, H. (2020). A Rate-Dependent Peridynamic Model for the Dynamic Behavior of Ceramic Materials. CMES-Computer Modeling in Engineering & Sciences, 124(1).

6. Dawaki, U. M., Dikko, A. U., Noma, S. S., & Aliyu, U. (2013). Heavy metals and physicochemical properties of soils in Kano urban agricultural lands. Nigerian Journal of Basic and Applied Sciences, 21(3), 239-246.

7. Deckers, S., Dondeyne, S., Vandekerckhoven, L., & Raes, D. (1995). Major soils and their formation in the West-African Sahel. Irrigated rice in the Sahel: Prospects for sustainable development, 23-35.

8. EPA, U. (2002). Supplemental guidance for developing soil screening levels for superfund sites, Appendix A—Generic SSLs for the residential and commercial/industrial scenarios. Washington DC: Office of Emergency and Remedial Response, United States Environmental Protection Agency, 9355-4.

9. Erdemir, A. (2005). Review of engineered tribological interfaces for improved boundary lubrication. Tribology International, 38(3), 249-256.

10. Estefan, G. (2013). Methods of soil, plant, and water analysis: a manual for the West Asia and North Africa region.

11. Eswaran, H., Lal, R., & Reich, P. F. (2001). Land degradation: an overview. Responses to Land Degradation. In Proc. 2nd International Conference on Land Degradation and Desertification. Khon Kaen, Thailand, edited by E. Bridges, I. Hannam, L. Oldeman, F. Penning de Vries, S. Scherr, and S. Sompatpanit. New Delhi: Oxford Press.

12. FAO/WHO. (2001). Food additives and contaminants. Joint Codex Alimentarius Commission. FAO/WHO Food Standards Programme, ALINORM 01/12A.

13. Gachot, C., Rosenkranz, A., Hsu, S. M., & Costa, H. L. (2017). A critical assessment of surface

texturing for friction and wear improvement. Wear, 372, 21-41.

14. Hengl, T., Leenaars, J. G., Shepherd, K. D., Walsh, M. G., Heuvelink, G. B., Mamo, T., ... & Kwabena, N. A. (2017). Soil nutrient maps of Sub-Saharan Africa: assessment of soil nutrient content at 250 m spatial resolution using machine learning. Nutrient Cycling in Agroecosystems, 109, 77-102.

15. Horneck, D. A., Sullivan, D. M., Owen, J. S., & Hart, J. M. (2011). Soil test interpretation guide.

16. Hunt, N., & Gilkes, R. (1992). Farm Monitoring Handbook–A practical down-toearth manual for farmers and other land users. University of Western Australia: Nedlands, WA, and Land Management Society: Como, WA.

17. Ibrahim, A. K., Usman, A., Abubakar, B., & Aminu, U. H. (2011). Extractable micronutrients status in relation to other soil properties in Billiri Local Government Area. Journal of Soil Science and Environmental Management, 3(10), 282-285.

18. Idera, F., Omotola, O., Adedayo, A., & Paul, U. J. (2015). Comparison of acid mixtures using conventional wet digestion methods for determination of heavy metals in fish tissues. J. Sci. Res. Rep, 8(7), 1-9.

19. Kabata-Pendias, A. (2000). Trace elements in soils and plants. CRC press.

20. Kihara, J., Bolo, P., Kinyua, M., Rurinda, J., & Piikki, K. (2020). Micronutrient deficiencies in African soils and the human nutritional nexus: opportunities with staple crops. Environmental Geochemistry and Health, 42, 3015-3033.20. Lal, R. (2006). Encyclopedia of Soil Science. Taylor and Francis, Florida, USA.

21. Lavado, R. S., & Porcelli, C. A. (2000). Contents and main fractions of trace elements in Typic Argiudolls of the Argentinean Pampas. Chemical Speciation & Bioavailability, 12(2), 67-70.

22. Liu, G., Simonne, E. H., & Li, Y. (2011). Nickel nutrition in plants. IFAS Extension University of Florida, 6.

23. Ma, Y., & Hooda, P. S. (2010). Chromium, nickel and cobalt. Trace elements in soils, 461-479.

24. Mao, B., Siddaiah, A., Liao, Y., & Menezes, P. L. (2020). Laser surface texturing and related techniques for enhancing tribological performance of engineering materials: A review. Journal of Manufacturing Processes, 53, 153-173.

25. McKenzie, N. N., Jacquier, D. D., Isbell, R. R., & Brown, K. K. (2004). Australian soils and landscapes: an illustrated compendium. CSIRO publishing.

26. Mulima, I. M., Shafiu, M., Ismaila, M., & Benisheikh, K. M. (2015). Status and Distribution of Some Available Micronutrients in Sudan and Sahel Savanna Agro-Ecological Zones of Yobe State, Nigeria. Journal of Environmental Issues and Agriculture in Developing Countries, 7(1), 18.

27. Mustapha, S., Voncir, N., Umar, S., & Abdulhamid, N. A. (2011). Status and Distribution of some Available Micronutrients in the Haplic usferts of Akko Local Government Area, Gombe State, Nigeria. International Journal of Soil Science, 6(4), 267.

28. Negasa, T., Ketema, H., Legesse, A., Sisay, M., & Temesgen, H. (2017). Variation in soil properties under different land use types managed by smallholder farmers along the toposequence in southern Ethiopia. Geoderma, 290, 40-50.

30. Obilor, A. F., Pacella, M., Wilson, A., & Silberschmidt, V. V. (2022). Micro-texturing of polymer surfaces using lasers: A review. The International Journal of Advanced Manufacturing Technology, 120(1-2), 103-135.

31. Ogundele, D. T., Adio, A. A., & Oludele, O. E. (2015). Heavy metal concentrations in plants and soil along heavy traffic roads in North Central Nigeria. Journal of Environmental & Analytical Toxicology, 5(6), 1.

32. Oluwadare, D. A., Voncir, N., Mustapha, S., & Mohammed, G. U. (2013). Evaluation and enhancement of available micronutrients status of cultivated soil of Nigeria guinea savanna using organic and inorganic amendments. IOSR Journal of Agriculture and Veterinary Science, 3(5), 62-68.

33. Oyinlola, E. Y., & Chude, V. O. (2010). Status of available micronutrients of the basement complex rock-derived alfisols in northern Nigeria savanna. Tropical and subtropical Agroecosystems, 12(2), 229-237.Tropical and Subtropical Agroecosystems, 12(2):229-237.

34. Patel, N. R., & Gohil, P. P. (2012). A review on biomaterials: scope, applications & human anatomy significance. Int. J. Emerg. Technol. Adv. Eng, 2(4), 91-101.

35. R Core Team, A., & R Core Team. (2022). R: A language and environment for statistical computing. R Foundation for Statistical Computing, Vienna, Austria. 2012.

36. Sarkar, P., De, D., & Rho, H. (2004). Synthesis and microstructural manipulation of ceramics by electrophoretic deposition. Journal of Materials Science, 39, 819-823.

37. Shukla, U. C., & Gupta, B. L. (1975). Response to Mn application and evaluation of chemical extractants to determine available Mn in some arid brown soils of Haryana (India). Journal of the Indian Society of Soil Science (India).

38. Singh, L., Sehgal, S., & Kuldeep, K. S. (2021). Behavior of Al2O3 in aluminum matrix composites: An overview. In E3S Web of Conferences (Vol. 309, p. 01028). EDP Sciences.

39. Srivastava, J. P., English, J. C., & Lal, R. (1993). Conserving soil moisture and fertility in the warm seasonally dry tropics. Washington, DC: World Bank.

40. Sundararajan, G., Joshi, S. V., & Krishna, L. R. (2016). Engineered surfaces for automotive engine and power train components. Current opinion in chemical engineering, 11, 1-6.

41. Tabi, F. O., & Ogunkunle, A. O. (2007). Spatial variation of some soil physico-chemical properties of an Alfisol in Southwestern Nigeria. Nigerian Journal of Soil and Environmental Research, 7, 82-91.

42. Tabor, N. J., Myers, T. S., & Michel, L. A. (2017). Sedimentologist's guide for recognition, description, and classification of paleosols. In Terrestrial depositional systems (pp. 165-208). Elsevier.

43. Tichy, J. A., & Meyer, D. M. (2000). Review of solid mechanics in tribology. International Journal of Solids and Structures, 37(1-2), 391-400.

44. Tilahun, G. (2007). Soil fertility status as influenced by different land uses in Maybar areas of South Wello Zone, North Ethiopia. Haramaya University, Ethiopia.

45. Ufot, U. O., Iren, O. B., & Chikere Njoku, C. U. (2016). Effects of land use on soil physical and chemical properties in Akokwa area of Imo State, Nigeria. International Journal of Life Sciences Scientific Research, 2(3), 273-278.

46. Weil, R. R. and Brady, N. C. (2017). Nature and Properties of Soils, 15th edition. Pearson Education, Inc. Delhi, India.

47. Yusuff, R. O., & Sonibare, J. A. (2004). Characterization of textile industries' effluents in Kaduna, Nigeria and pollution implications. Global nest: the int. J, 6(3), 212-221.

48. Zha, J. W., Dang, Z. M., Li, W. K., Zhu, Y. H., & Chen, G. (2014). Effect of micro-Si 3 N 4-nano-Al 2 O, sub> 3 co-filled particles on thermal conductivity, dielectric and mechanical properties of silicone rubber composites. IEEE Transactions on Dielectrics and Electrical Insulation, 21(4), 1989-1996.